Development of a 3D human osteoblast cell culture model for studying mechanobiology in orthodontics

Damien Brezulier, Pascal Pellen-Mussi, Sylvie Tricot-Doleux, Agnès Novella, Olivier Sorel, Sylvie Jeanne

Development of a 3D Human Osteoblast Cell Culture Model for Studying Mechanobiology in Orthodontics

Damien Brezulier[1,2], Pascal Pellen-Mussi[2], Sylvie Tricot-Doleux[2], Agnès Novella[2], Olivier Sorel[1], Sylvie Jeanne[1,2]

[1]Univ Rennes, CHU Rennes, Pole Odontologie, Rennes, France.
[2]ISCR, CNRS-UMR 6226, Rennes, France.

Summary:

Objectives: Mechanobiology phenomena constitute a major element of the cellular and tissue response during orthodontic treatment and the implantation of a biomaterial. Better understanding these phenomena will improve the effectiveness of our treatments. The objective of this work is to validate a model of three-dimensional (3D) culture of osteoblasts to study mechanobiology.

Materials/Methods: The hFOB 1.19 cell line was cultured either traditionally on a flat surface or in aggregates called spheroids. They were embedded in 0.8% low melting agarose type VII and placed in a PET transwell insert. Compressive forces of 1 g/cm² and 4 g/cm² were applied with an adjustable weight. Proliferation was evaluated by measuring diameters, monitoring glucose levels and conducting Hoechst/propidium iodide staining. ELISAs focusing on the pro-inflammatory mediators IL-6 and IL-8 and bone remodelling factor osteoprotegerin (OPG) were performed to evaluate soluble factor synthesis. qRT-PCR was performed to evaluate bone marker transcription.

Results: The 3D model shows good cell viability and permits interleukin dosing. Additionally, three gene expression profiles are analysable.

Limitations: The model allows analysis of conventional markers; larger exploration is needed for better understanding osteoblast mechanobiology. However, it only allows an analysis over 3 days.

Conclusion: The results obtained by applying constant compressive forces to 3D osteoblastic cultures validate this model system for exploring biomolecule release and analysing gene transcription. In particular, it highlights a disturbance in the expression of markers of osteogenesis.

Keywords: cell culture, mechanobiology, orthodontics, osteoblast

Introduction

Orthodontic tooth movement (OTM) is initiated by the interaction of cellular and molecular components of the periodontal ligament and alveolar bone (1). Conventional knowledge dictates that during OTM, the applied force leads to the creation of a compression side and a tension side. By convention, the tension side is marked by bone formation, whereas the compression side is marked by bone resorption. The applied orthodontic forces are transmitted *via* the stress of the extracellular matrix to the cells in alveolar bone and periodontal ligament. The transmission of this mechanical signal alters the vascularization of the periodontal ligament (2) and creates microcracks in bone (3). This leads to the local release of various molecules, such as neurotransmitters, cytokines, growth factors, colony-stimulating factors and arachidonic acid metabolites (4). The liberation of pro-inflammatory, angiogenic and osteogenic mediators triggers ligament and bone remodelling prior to OTM (5,6). The first phase during remodelling comprises the differentiation and activation of the precursors of osteoblasts and osteoclasts and is mediated by the release of interleukins IL-1, IL-6, IL-10, and IL-33; tumour necrosis factor alpha (TNFα) or the interferon IFNγ (7). During the second phase, the osteoclast differentiation is completed. It is controlled by the binding of receptor activator of nuclear factor kappa-B ligand (RANKL) on the RANK membrane receptor of pre-osteoclasts. In parallel, the decoy receptor to RANKL, called osteoprotegerin (OPG), shows decreased expression. In fact, compressive forces upregulate the RANKL/OPG ratio and promote osteoclast differentiation (8).

During bone remodelling, osteoblasts play a key role by regulating both resorption and formation (9). Osteoblasts transduce mechanical stimuli into biochemical signals through multiple mechanoreceptors, such as integrins, pericellular sensors, focal adhesions, ion channels, cadherins, connexins, and lipidic rafts (10). These proteins activate intracellular signalling cascades such as the MAPK, PI3K/Akt, GTPases, Wnt and calcium pathways to modulate osteoblastic differentiation by up- or downregulating gene expression (11). There is a need to better understand how all these mechanisms function. Osteoblasts also secrete bone matrix components before mineralization. The synthesized proteins reflect the stage of osteoblast differentiation, thus serving as phenotypic markers. Alkaline phosphatase (ALP) and collagen I (Col1) are commonly used as markers of phenotypes under mechanical stress (12). Col1 is a major structural protein of the bone matrix, whereas ALP is believed to reflect the first step of bone mineralization. In addition, the sequential development of bone depends on the transcription factor Runt-related transcription factor 2 (RunX2). Compressive forces have been shown to increase RunX2 expression (13). Col1 and ALP expression is observed at an early stage of cell differentiation (14). As the cells progress to the mineralization phase, peak levels of non-collagenous proteins are reached: osteopontin (OP) and osteocalcin (OCN) are expressed (15).

To better understand the changes taking place in bone during OTM, it is important to elucidate the cellular and molecular interactions within the bone tissue. The complexity of *in*

vivo studies makes analysing these communication channels difficult. As a result, models using cells isolated from alveolar bone have been established to simulate the application of orthodontic forces (16). Currently, cell culture is widely used in biomedical research to better elucidate the physiology, pathology and therapy of many processes and diseases. Much of our understanding of biological mechanisms such as migration, differentiation and force-sensing has been acquired from 2D (also called monolayer) cell culture (17). Although conventional 2D cell culture has predominated research fields, recent advancements in tissue engineering have allowed a shift towards culture using 3D structures (18). Regardless, the generic term "3D cell culture" actually covers a profound number of models, all of which have the characteristic of culturing cells within a matrix comprising poly-L-lactide acid, poly-lactic-co-glycolic acid, collagen, agarose, etc. The majority of these constructs are in fact isolated cells "standing up" in the scaffold (19). These authors suggest going further by integrating micro-tissues in the form of so-called spheroid cellular aggregates in an agarose matrix. The use of agarose matrices limits cellular attachment to the physiological extracellular matrix and therefore allows a strict evaluation of the role of mechanical compression without interference from the microenvironment.

In the field of orthodontics, the originally described 2D compression model (20) is still considered the gold standard. It is a simple method for the application of a static, compressive, unidirectional force on a cell layer. Conversely, 3D models are used to answer questions such as how do cells detect forces (mechano-sensing), how do cells convert mechanical stress into molecular signals (mechano-transduction), and how do these molecular signals influence the specific cellular response or to a specific force. Despite these possibilities, this 3D culture model requires strong validation before being included as a reference in the field.

The objective of this work was to validate a three-dimensional (3D) cell culture weight-based model to elucidate the complex cascade of secondary events to the application of various intensities of orthodontic forces.

1 Materials and methods

1.1 Cell culture

The human foetal osteoblastic cell line hFOB 1.19 (ATCC® CCL-11372™) was seeded at a density of $6x10^3$ cells/cm^2 in Dulbecco's modified Eagle medium (DMEM, Lonza, Belgium) mixed with Hams F12 (Lonza, Belgium) at a ratio of 1:1 and supplemented with 10% foetal bovine serum (Gibco, Life Technologies, UK), 2 mmol/L glutamine (Lonza, Belgium) and antibiotics (100 U/mL penicillin, 100 µg/mL streptomycin; Lonza, Belgium). The cells were cultured in a humidified atmosphere containing 5% CO_2 at a temperature of 34°C, during which time they were conditionally immortalized with a gene encoding a temperature-sensitive mutant (tsA58) of SV40 large T antigen (21). Upon reaching confluence, cells were passaged by trypsin/EDTA treatment (Lonza, Belgium).

1.1.1 2D model

Cells were resuspended in 0.8% low-melting agarose solution at a density of $4x10^5$ cells/mL for gene assays or $2x10^5$ cells/mL for protein assays. One millilitre of the solution was added into a 6-well transwell polyethylene terephthalate (PET) insert with a pore size 3 µm and a pore density of $8x10^5$ pores/cm^2 (Corning, Lowell, MA); the total gel thickness was 2 mm. The mixture was allowed to solidify for 20 min at room temperature. Then, 1.5 mL and 2.5 mL of medium were added to the upper and lower chambers of the well, respectively. Finally, a thin glass slide was placed on top of the agarose gel.

1.1.2 Spheroids

Flat-bottom 96-well microplates were treated with 50 µL of 1% agarose (Sigma-Aldrich, Saint-Louis, MO, USA) prepared in phosphate-buffered saline (Lonza, Belgium) to form a thin non-adhesive film to prevent cell adhesion (22). Cells were suspended at $1x10^4$ cells/mL and aliquots of 200 µL i.e. 2000 cells/well were seeded into individual wells to initiate spheroid formation, and the microplates were incubated at 34°C in a 5% CO_2 atmosphere. Cells were cultured in complete medium during spheroid growth that was not replaced. After 72 h of spheroid formation, each aggregate was collected by aspiration with a 100 µL pipette. After centrifugation at 800 rpm for 3 minutes, 96 or 192 spheroids were re-suspended in 1 mL of 0.8% agarose low melting solution type VII (Sigma-Aldrich, Saint Louis, MO, USA). Then, 1 mL of the solution was added into a 6-well transwell polyethylene terephthalate (PET) insert with a pore size of 3 µm and a pore density of $8x10^5$ pores/cm^2 in the membrane (Corning, Lowell, MA); the total gel thickness was 2 mm. The spheroid-agarose mixture was allowed to solidify for 20 min at room temperature. As previously described, 1.5 mL and 2.5 mL of medium were added to the upper and lower chambers of the well, respectively. Finally, a thin 22 mm diameter glass slide was placed on top of the spheroid-gel construct. Densities of 96 spheroids/mL for protein assays or 192 spheroids/mL for gene assays were used.

1.2 Static compressive force

In each of the two previous constructs, a static and unidirectional compressive force was applied. A plastic test tube cap was filled with lead pellets to adjust the weights. Based on the diameter of the glass slide that distributes the force over the agarose, the lead weight was adjusted to deliver forces of 1 g/cm^2 or 4 g/cm^2 (Fig. 1 and 2).

1.3 Cell survival and proliferation

1.3.1 Spheroid diameters

The increase in spheroid diameter was monitored by obtaining photographs via optical microscopy. The spheroids embedded in agarose were followed and compared to non-embedded spheroids constituting the control group. Collection of images at the standard 4x magnification allowed the use of a measurement layer in Photoshop CC software. Spheroids appeared round or ovoid; in the latter case, the largest diameter was retained.

1.3.2 Glucose consumption

The growth and vitality of the hFOB 1.19 cells embedded in an agarose matrix was assessed by the indirect measurement of metabolic activity (23). Each day, glucose uptake of the cells was measured in the medium with a cobas c 111 analyser (Roche Diagnostics GmbH, Allemagne). Based on the final volume of the solution, the cumulative amount of glucose consumed was calculated. Fresh culture medium without cells was used as a reference. Each test was done in triplicate.

1.3.3 Propidium iodide and Hoechst staining

Staining was performed using 5 µg/mL Hoechst 33258 and 1 µg/mL propidium iodide. The ratio between viable and dead cells was established as the ratio of both channel intensities. For the two-dimensional (2D) model, cells were incubated for 2 h at 34°C and analysed by confocal microscopy. A total of 5 pictures of each condition was analysed. For the 3D model, cells were incubated for 20 h incubation at 34°C with Hoechst, treated with propidium iodide 2 h before reading, and analysed by light sheet fluorescence microscopy. For each condition, between 3 and 6 spheroids were imaged and analysed.

1.4 RNA extraction and real-time PCR

Total RNA was extracted from hFOB 1.19 osteoblasts at 24 h and 72 h using a Nucleospin RNA extraction kit (Macherey Nagel, Germany), with some adaptations of the manufacturer's instructions with respect to the context of spheroids embedded in agarose matrix. The volume of reagent RA1 was multiplied by 2, i.e., increased to 700 µL.

Quantitative real-time PCR was carried out with a SYBR Green PCR kit (Applied Biosystems, Foster City, CA, USA) in an ABI Prism 7900 HT Fast system (Applied Biosystems) under the following cycling conditions: 2 min at 50°C; 10 min at 95°C; 40 cycles of 15 s at 95°C and 1 min at 60°C; and a final dissociation step. The primer sequences used in this experiment are listed in Table 1. The transcripts of the 18S and HPRT housekeeping gene were used normalize the mRNA levels (24,25). ~~As the same data were observed for these two housekeeping gene transcripts, HPRT results were only showed.~~ The results were normalized using the geometric mean Ct of HPRT and 18S. Quantitative results were analysed with SDS v2.3 software (Applied Biosystems). Relative gene expression was calculated with the $2^{-\Delta\Delta Ct}$ method (26). The assay for each gene was carried out in triplicate. The validation of the primers, the purity and integrity of the RNA, the amplification efficiency have been verified according to the recommendations of Taylor and Mrkusich (27).

1.5 Enzyme-linked immunosorbent assay

To determine the IL-6, IL-8 and OPG concentrations produced by hFOB 1.19 cells in response to mechanical compression, supernatants from 2D and 3D cell cultures were harvested, and the concentrations were measured by ELISA (DuoSet ELISA Development System Human IL-6, OPG and CXCL8, R&D Systems, Minneapolis, MN, USA) according to the manufacturer's

instructions. Supernatants were collected at 24 h and 72 h, and their absorbance at 450 nm was read with a spectrophotometer. Concentrations were calculated from the standard curves. Three independent experiments were performed for each condition.

1.6 Statistical analysis

Data analysis was performed with GraphPad Prism v6.0 (GraphPad Software, San Diego, CA, USA). Two-way ANOVA and Tukey's post-hoc tests were used to determine significant differences between groups. Data are expressed as the means ± SD, and differences were considered significant when $p<0.05$.

2 Results

2.1 Cell viability

Cell viability was checked in both models using two approaches. First, a metabolic- (glucose consumption over time) and optic-based (spheroid diameters) method was used. Over a period of 4 days, glucose consumption was maintained in both the 2D and 3D cultures indicating cellular viability; furthermore, the spheroid diameters stabilised over time as there was no statistically significant difference between the culture times for each stress intensity (Fig. 3).

The second approach consisted of the measurement of Hoechst 33258 staining, which labels viable cells, and propidium iodide staining, which labels dead cells. The Hoechst/IP ratio in the 2D model demonstrated constant viability at 24 h regardless of the compressive force exerted and a slightly reduced viability of 15% at 72 h at the highest pressure applied. In the spheroid model, at 24 h, the viability was significantly increased in response to the strongest compressive force and was not significantly decreased at 72 h in response to a pressure of 1 g/cm^2 (Fig. 4) (Supplemental data).

2.2 Expression of osteogenic markers

In the 2D model, *ALP* gene expression dropped significantly between 24 h and 72 h (-50%) (Fig. 5A), whereas in the 3D model, the opposite phenomenon was observed with a significant increase (+250%) in gene expression over time (Fig. 5B). At 72 h, ALP increased by a factor of 4 to 10 between the 2D and 3D models depending on the compressive force. The influence of the pressure exerted was more significant at 72 h in both cases. For the 2D model, the increase was correlated with the applied pressure (+40% for 1 g/cm^2 and +47% for 4 g/cm^2), but this increase was different for spheroids in which ALP expression peaked at 1 g/cm2 (+44% and +20% for 24 h and 72 h, respectively) but was negligible at 4 g/cm^2 ~~(<10%)~~.

In the 2D model, at 24 h, *COL1* expression gradually decreased with increased pressure exerted, whereas at 72 h, only the 4 g/cm^2 pressure caused a decrease of nearly 55% (Fig. 5C). In the 3D model, the expression remained constant regardless of the time under pressure or the pressure exerted (Fig. 5D).

OCN expression was almost constant at 24 h and 72 h in the 2D model (Fig. 5E). In contrast, it was significantly increased in the 3D model at 24 h and 72 h for the strongest pressure (≥80% compared to the control in both cases) ~~and at 72 h in proportion to the applied forces~~ (Fig. 5F).

OP expression decreased with pressure and time in the 2D model (Fig. 5G), with the largest decrease observed after the application of the largest force for three days (greater than 50% decrease). This reduction in expression depending of the pressure was less marked in the 3D model since the largest decrease recorded was only 23% at 24 h and no difference was detected at 72 h (Fig. 5H).

In the 2D model, *RunX2* expression was significantly modified ~~only at 72 h~~ in response to the strongest pressure applied (>150% compared to the control) (Fig. 5I). In the spheroid model, *RunX2* expression was significantly increased with the applied pressure at 24 h (+36% and +47%, respectively) and was significantly increased for the highest pressure at 72 h (+50%) (Fig. 5J).

2.3 Quantification of soluble factors

The release of IL-6 in the 2D model was low, with a peak value of 500 ng/mL, while in the 3D model, the release was 40 to 80 times higher. In the 2D model, the measured quantities were independent of applied pressure at 24 h and had doubled at 72 h in a pressure-dependent manner. In the 3D cultures, the IL-6 concentrations were very high and were proportional to the pressure applied twofold at 24 h, with larger quantities released at 72 h (+200%) (Fig. 6A and 6B).

Regarding the release of IL-8 in the 2D model, the measured quantities were low (approximately 400 ng/mL). The only significant value was at 72 h with a pressure of 4 g/cm2, where the amount of IL-8 was 10 times greater than that in the control. For spheroids, the values were significantly higher than those in the 2D cultures (from 11- to 40-fold). Unlike that observed with IL-6, there was no pressure-dependent effect, as no significant difference was highlighted. There was a time-dependent effect since the amount of IL-8 increased 250% at 72 h compared to the levels at 24 h (Fig. 6C and 6D).

For OPG, the difference was not marked as previously described in the 2D model and did not exceed a factor of 5 for each condition tested with amounts ranging from 133 to 1042 ng/mL. The quantity fluctuated little in response to pressure. Similarly, for the 3D culture, no significant difference was observed in response to the forces applied for 24 h and 72 h. The amount of protein was greater (+700%) after 3 days of pressure (Fig. 6E and 6F).

3 Discussion

Many cell lines are available to create culture models. However, we wanted to use a human line, closer to the clinical context. The hFOB 1.19, a human osteoblastic cell line was immortalized by transfected temperature sensitive SV40 T-antigen. This makes it possible to

free of the inter-individual variability of the primo-cultures. This line is closer to the healthy cell than the tumoral lines and allows suitable assays and comparison to others studies. In addition, the selected line allows the formation of spheroids, their embedding in agarose and mechanical stress application. We have control that the aggregates did not dissociate during the mechanical stressing. The hFOB 1.19 line appeared to be the most appropriate since its spheroids have a high rate of internal cohesion. Mechanical stress applied here were from $1g/cm^2$ to $4g/cm^2$. This is in the range of the most commonly applied forces in orthodontic weight-loaded approach models (16).

Micro-tissue constructs such as spheroids raise challenging questions such as control of the spatio-temporal distribution of nutrients and oxygen, the primary basis for cell viability and proliferation (18). Cell aggregates formed in a 3D culture create a gradient of nutrient access. The first validation step of the model was to control the viability of cells embedded in the agarose matrix. Conventional colorimetric methods based on the reduction of resazurin (Alamar blue assay) or tetrazolium (MTT assay) are indeed frequently used to evaluate viability in 2D cell culture. However, they are not applicable to spheroids. Tight cell-cell junctions can affect the absorption and diffusion kinetics of the dyes, thus modifying the reading of the test and making the results more difficult to interpret (28,29). To avoid the problem, we evaluated viability by monitoring diameters of the spheroids and indirectly by measuring the glucose uptake from the medium. In one hand, the diameter of the spheroids was not changed for the lowest pressures. On the other hand, for the most important pressure, the diameter increased strongly during the first hours then stabilized. This is explained by the loss of the spherical aspect of the aggregates in this condition in favour of an ogival aspect whose large diameter we have measured.

At the end of the 72 h compression period, glucose was still metabolized in both the 2D and 3D models. This result leads to the conclusion that hFOB 1.19 cells are still proliferating at this time regardless of the model used. This behaviour also indicates that the pore sizes of the insert membrane and matrix mesh are suitable for the exchange of nutrients and waste products between the two compartments. The surface of the spheroid aggregates exhibit the highest levels of proliferation, whereas the interior possesses the highest number of quiescent or necrotic cells (30). These data were also supported on our micro-tissues by light sheet fluorescence microscopy after labelling cells that had lost their membrane integrity with propidium iodide and living cells with Hoechst. Globally, glucose consumption and the use of fluorochromes confirmed preserved viability in spheroids compared to that of isolated cells embedded in agarose. These results are in agreement with those of previous studies (23,31).

A major limitation of culture in a matrix is the limited cell survival to 3 or 4 days. Only the poly-l-lactide matrix allows a longer follow-up, although limited to 2 weeks (32). This is why we did not carry out a follow-up on a longer term. In addition, our work focuses on the induction of tooth movement which take place during the first hours of application of orthodontic forces (3).

As several studies demonstrate their variation according to the mechanical stress imposed on cells, markers of osteoblastic activity were analysed by qRT-PCR (16). We used two reference genes according to the work of Vazquez and Rauh: 18S and HPRT (24,25). This is a different choice from Kirschneck's study which compares thirteen reference genes for the study of the consequences of dental movement on periodontal ligament fibroblasts (33). This is justified by a different culture model (3D versus 2D) and different cell populations (osteoblasts versus fibroblasts). The comparison of the gene expression between the 2D and 3D cell culture models revealed three situations:

1) There was no variation in the gene expression profile between the two models.
2) The expression of the markers was increased in the 3D model.
3) The expression was decreased in the 2D model but was maintained in the 3D model.

For the first observation, there was no difference in the expression profile between the two models with regard to *RunX2*, a master gene that transcriptionally promotes osteoblast differentiation. Its expression is essential for the homeostasis of bone tissue. This transcription factor has previously been shown to regulate the expression of various osteoblastic genes (34). In both model systems, its expression was increased in relation to the intensity and the duration of the pressure exerted. This confirms earlier works, such as Shen's study, which used murine osteoblasts embedded in a collagen matrix and reported that compressive stress ranging from 0 to 5 g/cm2 enhances osteoblastic differentiation (35).

In the case of *ALP* and *OCN*, the gene expression of both products was greatly increased in the spheroids compared to the 2D model. ALP is a very early marker of osteoblast differentiation and contributes to bone mineralization. Its expression was almost constant in the 2D cultures (no significant variations as a function of time or compressive force). In the 3D model, there was a difference between 24 h and 72 h of incubation with a maximum (x5 compared to the 24 h control) value observed at 1 g/cm^2. These results are consistent with those of the Elashry study, which demonstrated that 10 days of mechano-stimulation were needed to elicit a significant increase in *ALP* expression (30). Other studies confirm the increase in the expression of ALP in the spheroid model (36). This increase is also observed in saliva during orthodontic treatment (37). This expression is due to both mechanical and genetic factors: the interaction of osteoblasts in 3D space and tension within the spheroids.

It is well known that the *OCN* gene, as a target of β-catenin, plays a decisive role in osteogenesis. Therefore, the expression of genes involved in the *Wnt/*β-catenin pathway contributes to spheroid formation (38,39). The expression of the *OCN* gene is characteristic of the late stages of osteoblastic differentiation. Osteocalcin, the most abundant non-collagenous protein in bone, can be considered a signal that recruits fuses osteoclastic progenitors until they mature (40). Hoang demonstrated the ability of this protein to bind hydroxyapatite crystals and to inhibit their growth (41). On the one hand, its expression is almost constant in the 2D model regardless of the time and the compressive force applied. On the other hand, its expression was clearly increased with time in the 3D model and peaked in response to the highest compressive force. This is in agreement with results in the

literature reporting that OCN is increased during orthodontic treatment *in vivo* (7) as well as *in vitro* (42).

In the last experiment, *Col1* and *OP* gene expression levels decreased as a function of time and pressure applied in the 2D model but were constant in the 3D model. Col1 is a marker of the later stages of osteoblastic differentiation. Its expression decreased proportionally to the weight applied in the 2D model at 24 h and remained low at 72 h. Regarding spheroids, neither time nor force applied had an impact on Col1 expression. Many studies have demonstrated the induction of collagen expression by mechanical forces (12,43). However, Min reported that the mechano-response of fibroblasts varies according to the force applied: gene induction with weak compression and deactivation with stronger forces (44). In spheroids, the abundance of intercellular junctions allows the distribution of the force exerted to all the cells, unlike the cells isolated in agarose matrix (39). This could explain the decrease in collagen expression in the 2D model and the consistent gene expression in the 3D model. *OP* gene expression was significantly diminished as a function of time and pressure exerted in the 2D model, while its expression was almost constant in the 3D model. As described by Singh, OP is a molecule released by osteoblasts and acts as a signal for the recruitment, differentiation and attachment of osteoclasts (45). This phenomenon allows for the degradation of the non-mineralized matrix and characterizes the later stages of osteoblastic differentiation. OP has been shown to have a regulatory effect on hydroxyapatite crystal growth and potently inhibits the mineralization of osteoblast cultures in a phosphate-dependent manner. Bone remodelling is vital for OTM (46); thus, it is crucial that OP expression be maintained regardless of the forces applied and the time of application (45). Some authors showed the increase in its concentration on the compression side from the initiation of the OTM *in vivo* with a peak reached on the second day after initiating pressure. Following the increase in the expression of OPN, the number of osteoclasts increased 17-fold compared to the control, and numerous resorption depressions were observed on the pressure side of the alveolar bone (47).

Regarding the release of IL-6 and IL-8, in this study, a temporal effect between 24 h and 72 h was observed in both models. These cytokines are characteristic of the inflammatory response and osteoblastic activity. Moreover, these markers of osteoblast activity are usually found in the crevicular fluid of teeth subjected to OTM (4).

IL-6, which is produced by various cells in the medullary microenvironment (including monocytes, fibroblasts and T cells), is an important regulator of osteoclast formation *in vivo* (48). It is also produced by osteoblasts and induces bone resorption both alone and in concert with other bone resorption agents (49). Although one study found that compressive forces have little impact on alveolar bone cells in 2D culture models (50), other studies demonstrated that static compressive forces promote IL-6 release in similar models (51,52). In our study, the quantities of IL-6 collected in the 3D model were 40 times higher than those collected in the 2D model. The increase in IL-6 release in the 3D model could be explained by

a model effect: spheroidal culture leads to increased transcription of interleukins (48), and IL-6 expression is greatly enhanced by mechanical stimulation (53).

IL-8 stimulates both osteoclastogenesis and bone resorption in human osteoclasts derived from peripheral blood mononuclear cells. It also regulates the expression of the essential osteoclastogenic factor RANKL (54). Similar to IL-6, IL-8 was released in greater quantities in the 3D model. In the 2D model, its release was very low at 24 h but had increased at 72 h. These results agree with those of another study showing that IL-8 expression was only modulated by the application of compressive forces ranging from 0.5 to 3 g/cm2 during the first 24 h (55).

Finally, it has been shown that OPG plays a key role in RANK/RANKL coupling. OPG is a soluble cytokine that inhibits osteoclastogenesis via its endogenous antagonist activity that neutralizes the biological effects of RANKL and therefore acts as an inhibitor of bone resorption. The biological effects of OPG on bone cells include inhibition of the terminal stages of osteoclast differentiation, suppression of mature osteoclast activation and induction of apoptosis. It is obvious that the RANKL/OPG interaction plays a crucial role during tooth movement. An elevated RANKL/OPG ratio in the gingival fluid of displaced teeth has been demonstrated (8). In this study, OPG expression in the 2D model was almost non-existent at 24 h and was weak at 72 h. In the 3D model, the released quantities at 72 h were seven times higher than those at 24 h. The results showed that the quantities of OPG released were only weakly dependent on the compressive forces applied in the two models and that in both models, the strongest pressure induced a decrease in OPG release. These results are consistent with those conducted on bone cell lines (56). However, other authors have shown that OPG expression is clearly upregulated at both the mRNA and protein levels when cells were exposed to mechanical stimuli (57). However, it should be noted that these studies used mesenchymal stem cells and not osteoblasts.

Conclusion

In this study, a 3D model was developed to measure the impact of mechanical stress on osteoblasts. The results showed that cell viability and metabolism were conserved; however, differences in responses to mechanical stimuli were observed between 2D and 3D cultures. Indeed, there is a proportionality in the responses in the spheroids that is a time- and pressure-dependent in terms of the expression of osteogenesis markers and the release of cytokines. Spheroids are comparable to micro-tissues, and the results obtained in this study are more reminiscent to *in vivo* physiology than 2D models. It is therefore a seductive and more realistic approach to studying bone mechanobiology.

Conflict of interest: none

Ethical approval human and animal experiments: human commercial cells were used according to the Laboratory accreditation DC-2012-1573.

Acknowledgements:
The authors acknowledge the members of the Microscopy XXXX Imaging Center (XXX), in particular, Drs X. Pinson and S. Dutertre. They also acknowledge the Biochemistry-Toxicology Laboratory of the University Hospital of Rennes, Pr C. Bendavid and Dr M. Bourgeois.

Funding sources:

This work was supported by the French Society of Orthodontics and Dento Facial Orthopedics (SFODF); the National Institute for Medical Research (INSERM) and the French Federation of Orthodontics (FFO).

References:

1. Isola G, Matarese G, Cordasco G, Perillo L, Ramaglia L. Mechanobiology of the tooth movement during the orthodontic treatment: a literature review. Minerva Stomatol. 2016 Mar 17;

2. Schwarz AM. Tissue changes incidental to orthodontic tooth movement. Int J Orthod Oral Surg Radiogr. 1932 Apr 1;18(4):331–52.

3. Henneman S, Von den Hoff JW, Maltha JC. Mechanobiology of tooth movement. Eur J Orthod. 2008 Jun 1;30(3):299–306.

4. Krishnan V, Davidovitch Z. Cellular, molecular, and tissue-level reactions to orthodontic force. Am J Orthod Dentofac Orthop Off Publ Am Assoc Orthod Its Const Soc Am Board Orthod. 2006 Apr;129(4):469.e1-32.

5. Feller L, Khammissa R a. G, Schechter I, Thomadakis G, Fourie J, Lemmer J. Biological Events in Periodontal Ligament and Alveolar Bone Associated with Application of Orthodontic Forces. ScientificWorldJournal. 2015;2015:876509.

6. Masella RS, Meister M. Current concepts in the biology of orthodontic tooth movement. Am J Orthod Dentofac Orthop Off Publ Am Assoc Orthod Its Const Soc Am Board Orthod. 2006 Apr;129(4):458–68.

7. Vansant L, Cadenas De Llano-Pérula M, Verdonck A, Willems G. Expression of biological mediators during orthodontic tooth movement: A systematic review. Arch Oral Biol. 2018 Nov 1;95:170–86.

8. Yamaguchi M. RANK/RANKL/OPG during orthodontic tooth movement. Orthod Craniofac Res. 2009 May;12(2):113–9.

9. Tripuwabhrut P, Mustafa M, Gjerde CG, Brudvik P, Mustafa K. Effect of compressive force on human osteoblast-like cells and bone remodelling: An in vitro study. Arch Oral Biol. 2013 Jul;58(7):826–36.

10. Brézulier D, Pellen-Mussi P, Sorel O, Jeanne S. La mécanobiologie osseuse, un domaine émergeant : revue de littérature. Orthod Fr. 2018 Dec 1;89(4):343–53.

11. Miyashita S, Ahmed NEMB, Murakami M, Iohara K, Yamamoto T, Horibe H, et al. Mechanical forces induce odontoblastic differentiation of mesenchymal stem cells on three-dimensional biomimetic scaffolds: Mechanical forces induce odontoblastic differentiation of MSCs. J Tissue Eng Regen Med. 2017 Feb;11(2):434–46.

12. Pavlin D, Dove SB, Zadro R, Gluhak-Heinrich J. Mechanical Loading Stimulates Differentiation of Periodontal Osteoblasts in a Mouse Osteoinduction Model: Effect on Type I Collagen and Alkaline Phosphatase Genes. Calcif Tissue Int. 2000 Aug;67(2):163–72.

13. Baumert U, Golan I, Becker B, Hrala BP, Redlich M, Roos HA, et al. Pressure simulation of orthodontic force in osteoblasts: a pilot study. Orthod Craniofac Res. 2004 Feb 1;7(1):3–9.

14. Wlodarski KH, Reddi AH. Alkaline phosphatase as a marker of osteoinductive cells.

Calcif Tissue Int. 1986 Dec;39(6):382–5.

15. Lian JB, Stein GS. Development of the osteoblast phenotype: molecular mechanisms mediating osteoblast growth and differentiation. Iowa Orthop J. 1995;15:118–40.

16. Janjic M, Docheva D, Trickovic Janjic O, Wichelhaus A, Baumert U. In Vitro Weight-Loaded Cell Models for Understanding Mechanodependent Molecular Pathways Involved in Orthodontic Tooth Movement: A Systematic Review [Internet]. Stem Cells International. 2018 [cited 2018 Oct 30]. Available from: https://www.hindawi.com/journals/sci/2018/3208285/

17. Baker BM, Chen CS. Deconstructing the third dimension – how 3D culture microenvironments alter cellular cues. J Cell Sci. 2012 Jul 1;125(13):3015–24.

18. Duval K, Grover H, Han L-H, Mou Y, Pegoraro AF, Fredberg J, et al. Modeling Physiological Events in 2D vs. 3D Cell Culture. Physiology. 2017 Jul;32(4):266–77.

19. Yang L, Yang Y, Wang S, Li Y, Zhao Z. In vitro mechanical loading models for periodontal ligament cells: From two-dimensional to three-dimensional models. Arch Oral Biol. 2015 Mar;60(3):416–24.

20. Kanai K. Initial effects of continuously applied compressive stress to human periodontal ligament fibroblasts. J Jpn Orthod Soc. 1992;51:153–63.

21. Harris SA, Enger RJ, Riggs LB, Spelsberg TC. Development and characterization of a conditionally immortalized human fetal osteoblastic cell line. J Bone Miner Res. 1995 Feb 1;10(2):178–86.

22. Friedrich J, Seidel C, Ebner R, Kunz-Schughart LA. Spheroid-based drug screen: considerations and practical approach. Nat Protoc. 2009 Mar;4(3):309–24.

23. Detsch R, Alles S, Hum J, Westenberger P, Sieker F, Heusinger D, et al. Osteogenic differentiation of umbilical cord and adipose derived stem cells onto highly porous 45S5 Bioglass®-based scaffolds. J Biomed Mater Res A. 2015 Mar;103(3):1029–37.

24. Rauh J, Jacobi A, Stiehler M. Identification of Stable Reference Genes for Gene Expression Analysis of Three-Dimensional Cultivated Human Bone Marrow-Derived Mesenchymal Stromal Cells for Bone Tissue Engineering. Tissue Eng Part C Methods. 2015 Feb 1;21(2):192–206.

25. Vazquez M, Evans BAJ, Riccardi D, Evans SL, Ralphs JR, Dillingham CM, et al. A New Method to Investigate How Mechanical Loading of Osteocytes Controls Osteoblasts. Front Endocrinol [Internet]. 2014 [cited 2019 Dec 19];5. Available from: https://www.frontiersin.org/articles/10.3389/fendo.2014.00208/full

26. Livak KJ, Schmittgen TD. Analysis of Relative Gene Expression Data Using Real-Time Quantitative PCR and the 2−ΔΔCT Method. Methods. 2001 Dec 1;25(4):402–8.

27. Taylor SC, Mrkusich EM. The State of RT-Quantitative PCR: Firsthand Observations of Implementation of Minimum Information for the Publication of Quantitative Real-Time PCR Experiments (MIQE). J Mol Microbiol Biotechnol. 2014;24(1):46–52.

28. Kijanska M, Kelm J. In vitro 3D spheroids and microtissues: ATP-based cell viability and toxicity assays. 2016;

29. Walzl A, Unger C, Kramer N, Unterleuthner D, Scherzer M, Hengstschläger M, et al. The Resazurin Reduction Assay Can Distinguish Cytotoxic from Cytostatic Compounds in Spheroid Screening Assays. J Biomol Screen. 2014 Aug 1;19(7):1047–59.

30. Edmondson R, Broglie JJ, Adcock AF, Yang L. Three-Dimensional Cell Culture Systems and Their Applications in Drug Discovery and Cell-Based Biosensors. ASSAY Drug Dev Technol. 2014 May;12(4):207–18.

31. Cheng G, Tse J, Jain RK, Munn LL. Micro-Environmental Mechanical Stress Controls Tumor Spheroid Size and Morphology by Suppressing Proliferation and Inducing Apoptosis in Cancer Cells. Blagosklonny MV, editor. PLoS ONE. 2009 Feb 27;4(2):e4632.

32. Liao W, Okada M, Sakamoto F, Okita N, Inami K, Nishiura A, et al. In vitro human periodontal ligament-like tissue formation with porous poly-l-lactide matrix. Mater Sci Eng C. 2013 Aug 1;33(6):3273–80.

33. Kirschneck C, Batschkus S, Proff P, Köstler J, Spanier G, Schröder A. Valid gene expression normalization by RT-qPCR in studies on hPDL fibroblasts with focus on orthodontic tooth movement and periodontitis. Sci Rep. 2017 Nov 7;7(1):1–13.

34. Ducy P, Zhang R, Geoffroy V, Ridall AL, Karsenty G. Osf2/Cbfa1: A Transcriptional Activator of Osteoblast Differentiation. Cell. 1997 May 30;89(5):747–54.

35. Shen X-Q, Geng Y-M, Liu P, Huang X-Y, Li S-Y, Liu C-D, et al. Magnitude-dependent response of osteoblasts regulated by compressive stress. Sci Rep. 2017 20;7:44925.

36. Moritani Y, Usui M, Sano K, Nakazawa K, Hanatani T, Nakatomi M, et al. Spheroid culture enhances osteogenic potential of periodontal ligament mesenchymal stem cells. J Periodontal Res. 2018;53(5):870–82.

37. Al-Khatieeb MM, Rafeeq RA, Saleem AI. Relationship Between Orthodontic Force Applied by Monoblock and Salivary Levels of Alkaline Phosphatase and Lactate Dehydrogenase Enzymes. J Contemp Dent Pract. 2018 Nov 1;19(11):1346–51.

38. Vincan E, Schwab RHM, Flanagan DJ, Moselen JM, Tran BM, Barker N, et al. Chapter Ten - The Central Role of Wnt Signaling and Organoid Technology in Personalizing Anticancer Therapy. In: Larraín J, Olivares G, editors. Progress in Molecular Biology and Translational Science [Internet]. Academic Press; 2018 [cited 2019 Jun 4]. p. 299–319. (WNT Signaling in Health and Disease; vol. 153). Available from: http://www.sciencedirect.com/science/article/pii/S1877117317301874

39. Marie PJ, Haÿ E. Cadherins and Wnt signalling: a functional link controlling bone formation. BoneKEy Rep [Internet]. 2013 Apr 17 [cited 2019 Jan 14];2. Available from: https://www.ncbi.nlm.nih.gov/pmc/articles/PMC3722765/

40. Neve A, Corrado A, Cantatore FP. Osteocalcin: skeletal and extra-skeletal effects. J Cell Physiol. 2013 Jun;228(6):1149–53.

41. Hoang QQ, Sicheri F, Howard AJ, Yang DSC. Bone recognition mechanism of

porcine osteocalcin from crystal structure. Nature. 2003 Oct 30;425(6961):977–80.

42. Shunzhi Y, Zhonghai L, Ning Y. Mechanical stress affects the osteogenic differentiation of human ligamentum flavum cells via the BMP-Smad1 signaling pathway. Mol Med Rep. 2017 Nov;16(5):7692–8.

43. Redlich M, Palmon A, Zaks B, Geremi E, Rayzman S, Shoshan S. The effect of centrifugal force on the transcription levels of collagen type I and collagenase in cultured canine gingival fibroblasts. Arch Oral Biol. 1998 Apr 1;43(4):313–6.

44. Min J, Li B, Liu C, Guo W, Hong S, Tang J, et al. Extracellular matrix metabolism disorder induced by mechanical strain on human parametrial ligament fibroblasts. Mol Med Rep. 2017 May;15(5):3278–84.

45. Singh A, Gill G, Kaur H, Amhmed M, Jakhu H. Role of osteopontin in bone remodeling and orthodontic tooth movement: a review. Prog Orthod. 2018 Jun 25;19(1):18.

46. Nomura S, Takano-Yamamoto T. Molecular events caused by mechanical stress in bone. Matrix Biol. 2000 May 1;19(2):91–6.

47. Terai K, Takano-Yamamoto T, Ohba Y, Hiura K, Sugimoto M, Sato M, et al. Role of Osteopontin in Bone Remodeling Caused by Mechanical Stress. J Bone Miner Res. 1999;14(6):839–49.

48. Kurihara N, Bertolini D, Suda T, Akiyama Y, Roodman GD. IL-6 stimulates osteoclast-like multinucleated cell formation in long term human marrow cultures by inducing IL-1 release. J Immunol. 1990 Jan 6;144(11):4226–30.

49. Ishimi Y, Miyaura C, Jin CH, Akatsu T, Abe E, Nakamura Y, et al. IL-6 is produced by osteoblasts and induces bone resorption. J Immunol. 1990 Nov 15;145(10):3297–303.

50. Shi J, Baumert U, Folwaczny M, Wichelhaus A. Influence of static forces on the expression of selected parameters of inflammation in periodontal ligament cells and alveolar bone cells in a co-culture in vitro model. Clin Oral Investig [Internet]. 2018 Oct 15 [cited 2018 Oct 27]; Available from: https://doi.org/10.1007/s00784-018-2697-2

51. Tripuwabhrut P, Mustafa K, Brudvik P, Mustafa M. Initial responses of osteoblasts derived from human alveolar bone to various compressive forces. Eur J Oral Sci. 2012 Aug;120(4):311–8.

52. Asano M, Yamaguchi M, Nakajima R, Fujita S, Utsunomiya T, Yamamoto H, et al. IL-8 and MCP-1 induced by excessive orthodontic force mediates odontoclastogenesis in periodontal tissues. Oral Dis. 2011 Jul;17(5):489–98.

53. Wang X, Fan J, Zhang M, Sun Z, Xu G. Gene expression changes under cyclic mechanical stretching in rat retinal glial (Müller) cells. PloS One. 2013;8(5):e63467.

54. Bendre MS, Montague DC, Peery T, Akel NS, Gaddy D, Suva LJ. Interleukin-8 stimulation of osteoclastogenesis and bone resorption is a mechanism for the increased osteolysis of metastatic bone disease. Bone. 2003 Jul;33(1):28–37.

55. Koyama Y, Mitsui N, Suzuki N, Yanagisawa M, Sanuki R, Isokawa K, et al. Effect of

compressive force on the expression of inflammatory cytokines and their receptors in osteoblastic Saos-2 cells. Arch Oral Biol. 2008 May;53(5):488–96.

56. Grimm S, Walter C, Pabst A, Goldschmitt J, Wehrbein H, Jacobs C. Effect of compressive loading and incubation with clodronate on the RANKL/OPG system of human osteoblasts. J Orofac Orthop Fortschritte Kieferorthopädie. 2015 Nov 1;76(6):531–42.

57. Zhang L, Liu W, Zhao J, Ma X, Shen L, Zhang Y, et al. Mechanical stress regulates osteogenic differentiation and RANKL/OPG ratio in periodontal ligament stem cells by the Wnt/β-catenin pathway. Biochim Biophys Acta BBA - Gen Subj. 2016 Oct 1;1860(10):2211–9.

Figure legends:

Figure 1: Illustrations of the cell culture models for mechanical stress applications.

Figure 2: Clinical photo of the setup. General overview (A) and focus on the weight resting on the agarose matrix placed at the bottom of the insert (B).

Figure 3: Cumulative glucose uptake of hFOB 1.19 cells cultivated for 96 h under various compressive weights in a 2D culture (A) and a 3D spheroid culture (B). Monitoring of spheroid diameters under compressive strain (C).

Figure 4: (A) Hoechst/PI ratio based on immunohistochemical staining as recorded by confocal microscopy for 2D culture and (C) images of cells in the 2D model after 72 h of compressive stress. (B) Light sheet fluorescence microscopy for 3D culture and (D) images of spheroids after 72 h of compressive stress. (*$p < 0.05$ compared to 0 g/cm^2).

Figure 5: qRT-PCR demonstrating the effect of different magnitudes of compressive force for 24 h or 72 h on the mRNA expression of *ALP* (A and B), *Col1* (C and D), *OCN* (E and F), *OP* (G and H) and *Runx2* (I and J) relative to that of the endogenous control (HPRT). Numbers are presented as the mean and SEM (*$p < 0.05$ compared to 0 g/cm^2, # $p < 0.05$ compared to 1 g/cm^2).

Figure 6: Effect of varying magnitudes of compressive force on the protein expression of IL-6 (A and B), IL-8 (C and D) and OPG (E and F) after 24 h or 72 h of compressive force. The experiments were performed in triplicate. Numbers are presented as the mean and SEM.

Table 1: Description and characteristics of primers used for real-time PCR.

Supplemental data: Exploration by light sheet microscopy of a spheroid grown in an agarose matrix and compressed by a force of 4 g/cm^2 for 72 hours. The staining performed here is Hoechst 33258 (blue) and propidium iodide (red).

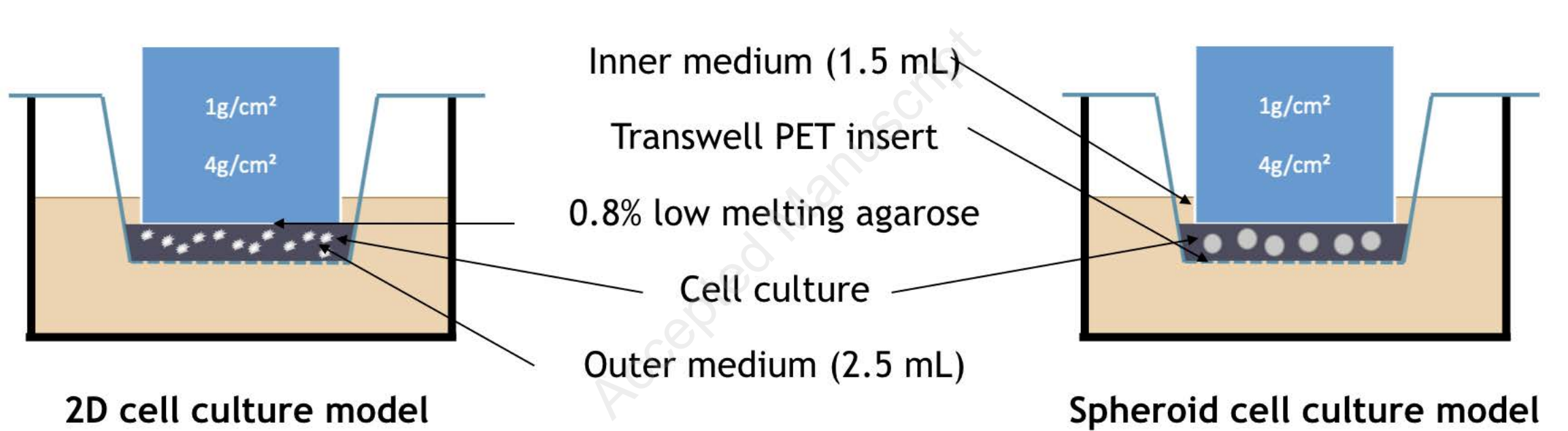

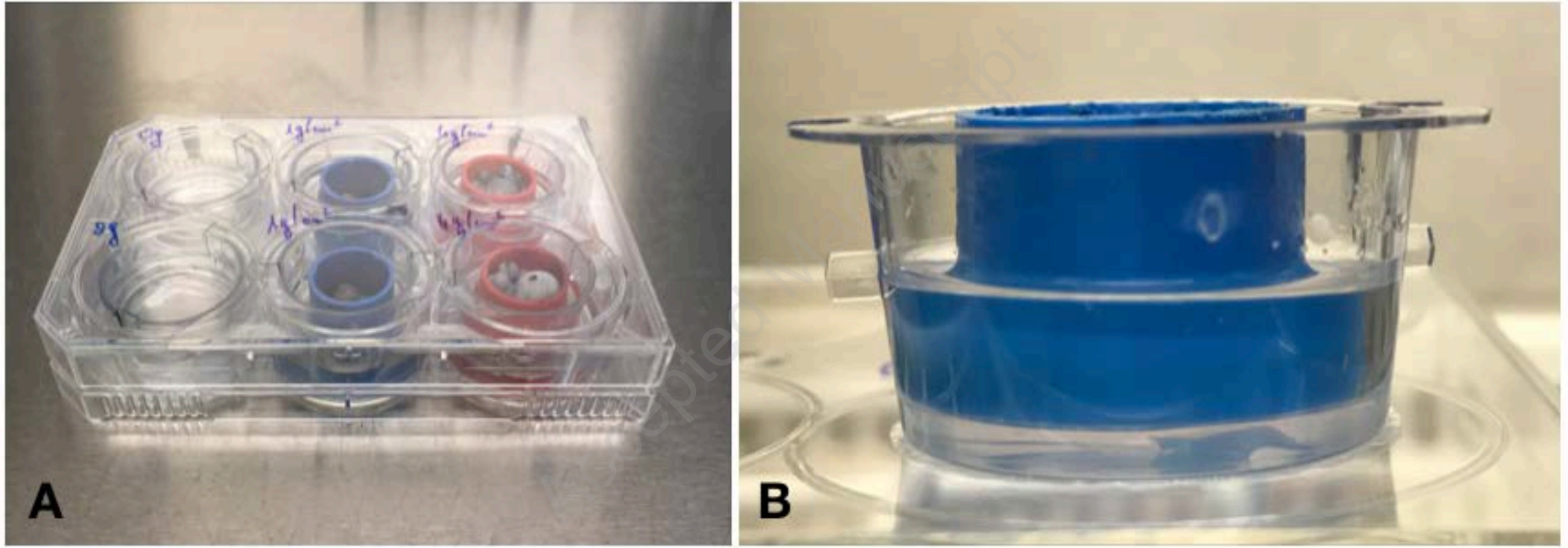
A
B

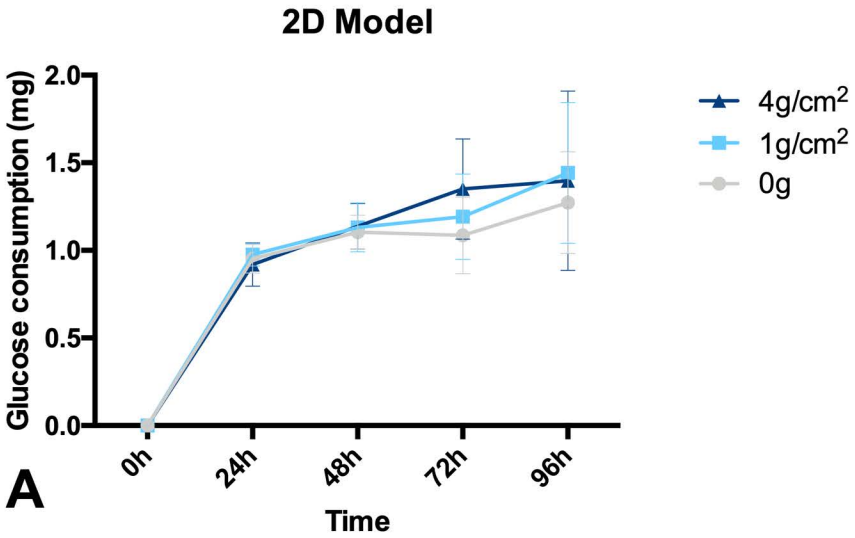

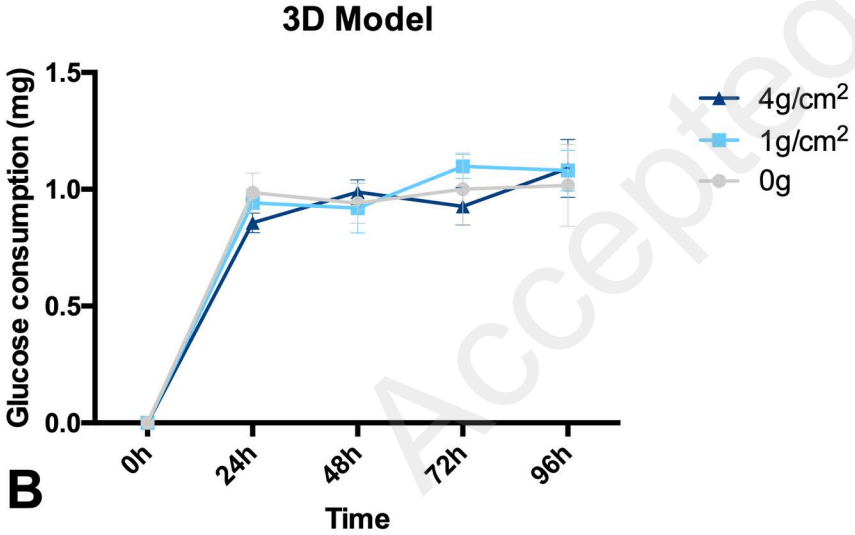

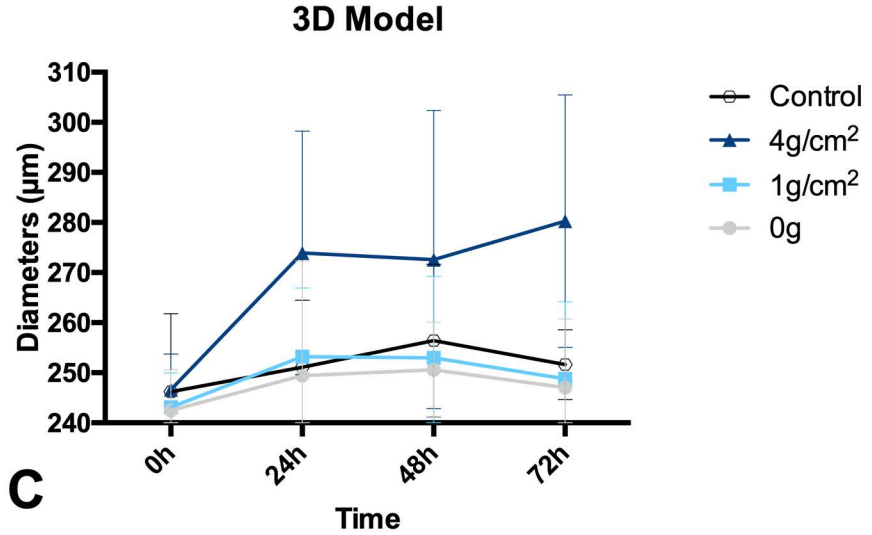

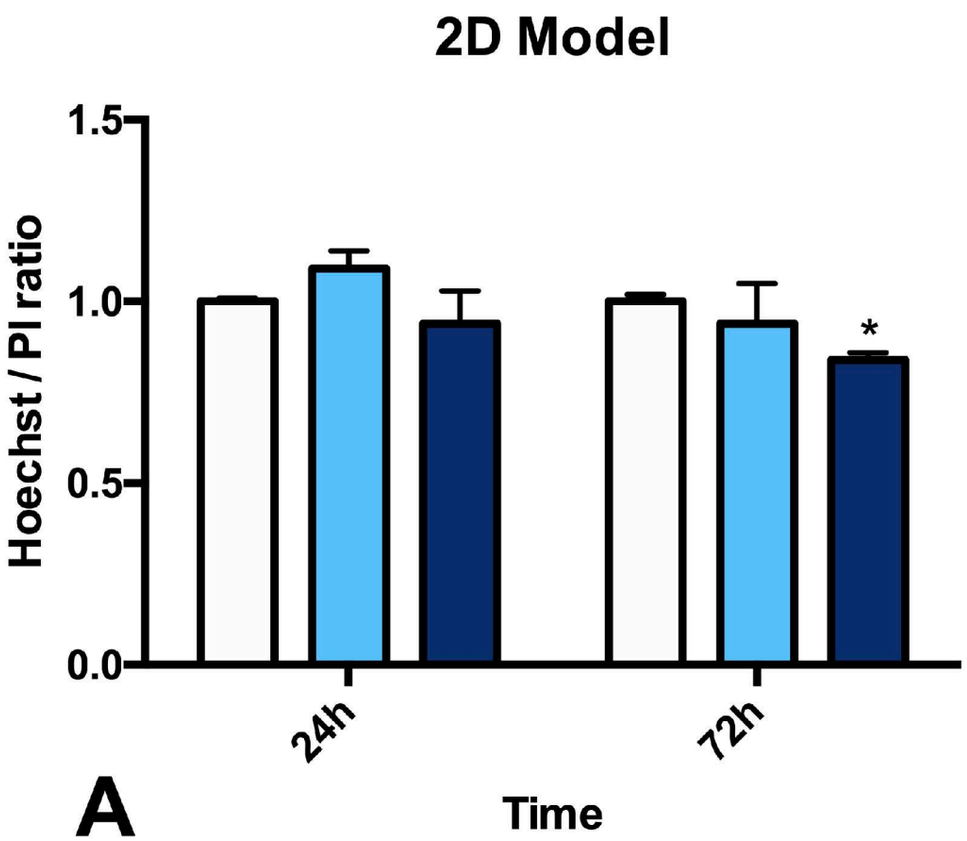

A

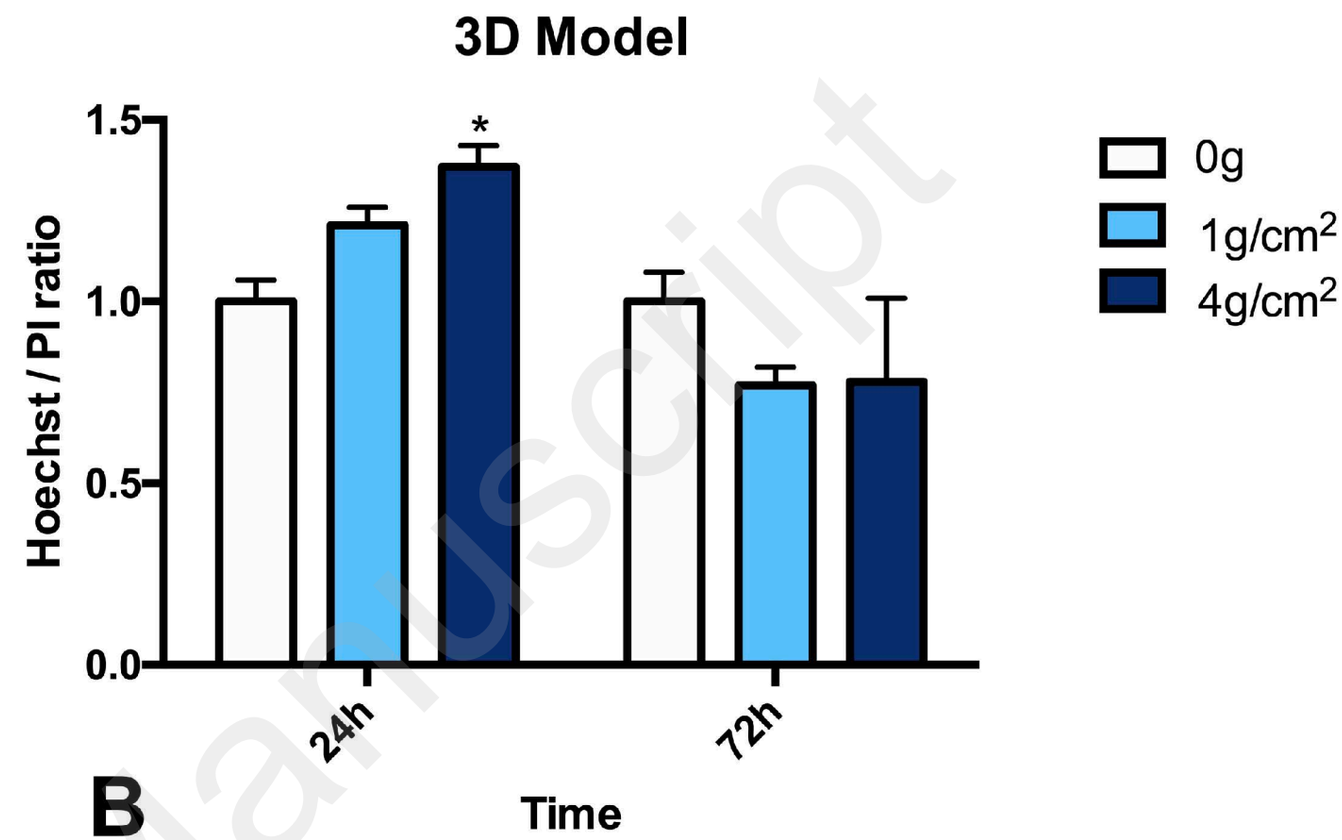

B

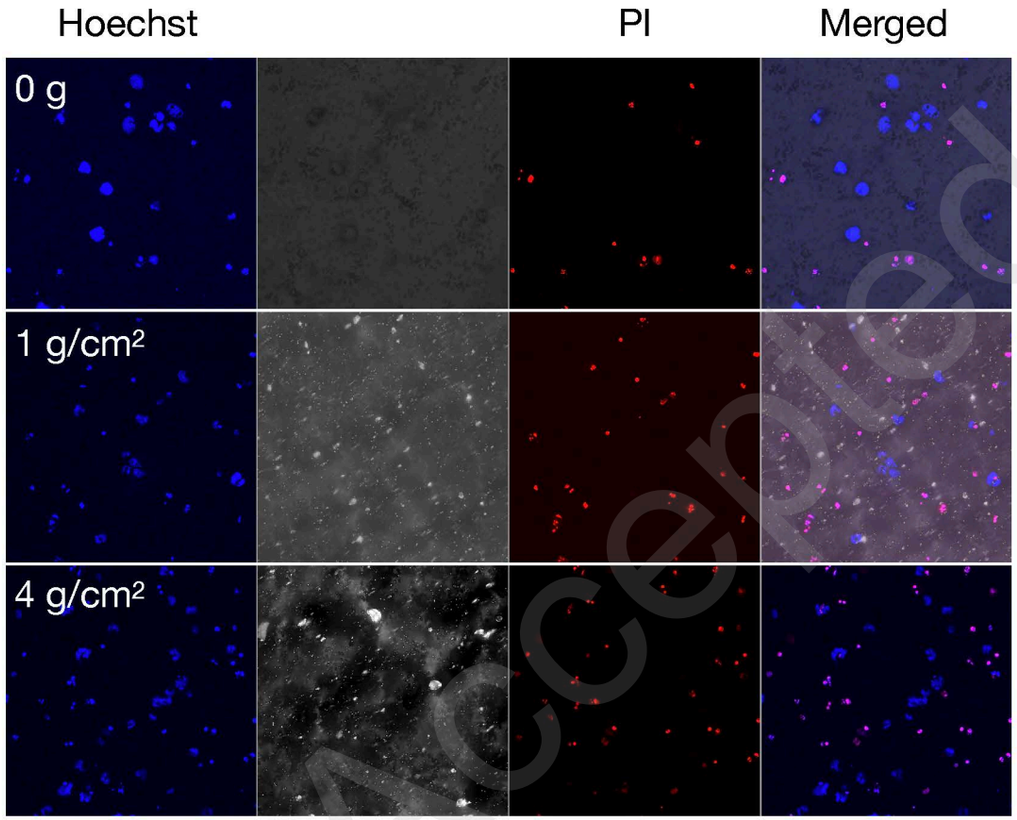

C

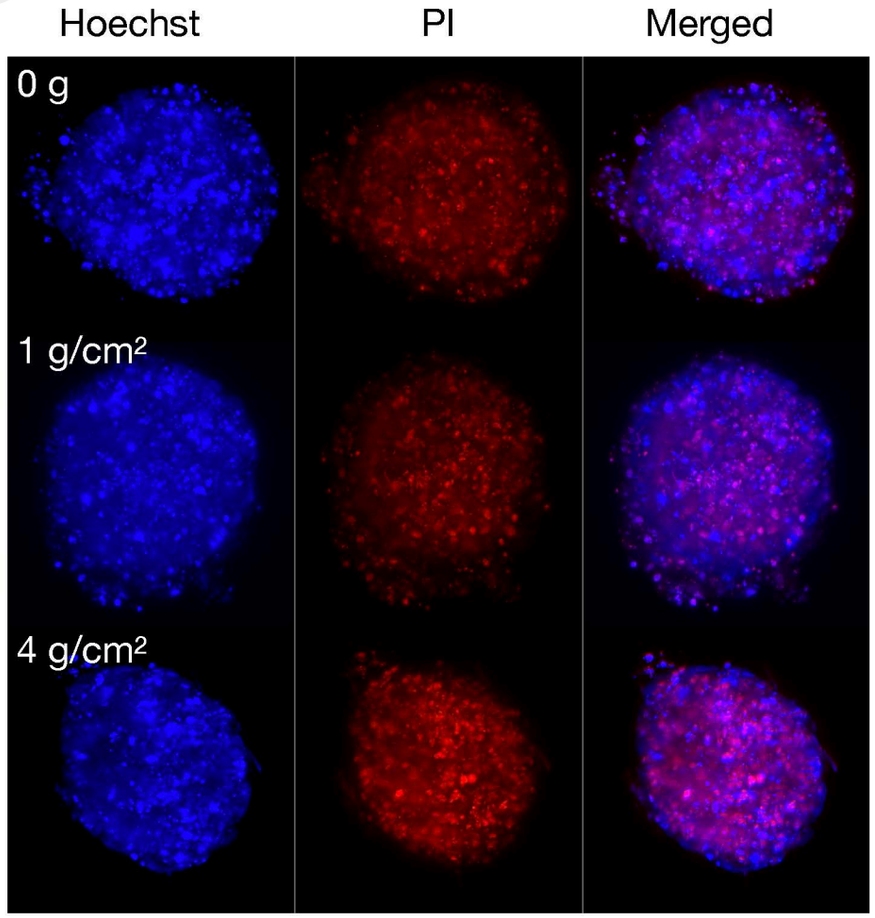

D